



ELSEVIER

Journal of Nuclear Materials 283–287 (2000) 952–956

**Journal of  
nuclear  
materials**

www.elsevier.nl/locate/jnucmat

# Cation disordering in magnesium aluminate spinel crystals induced by electron or ion irradiation

Takeshi Soeda <sup>a,\*</sup>, Syo Matsumura <sup>a</sup>, Chiken Kinoshita <sup>a</sup>, Nestor J. Zaluzec <sup>b</sup><sup>a</sup> Department of Applied Quantum Physics and Nuclear Engineering, Kyushu University, Hakozaki, Fukuoka 812-8581, Japan<sup>b</sup> Materials Science Division, Argonne National Laboratory, 9700 South Cass Avenue, Argonne, IL 60439, USA

## Abstract

Structural changes in magnesium aluminate spinel ( $\text{MgO} \cdot n\text{Al}_2\text{O}_3$ ) single crystals, which were irradiated with 900 keV electrons or 1 MeV  $\text{Ne}^+$  ions at 873 K, were examined by electron channeling enhanced X-ray microanalysis. Unirradiated  $\text{MgO} \cdot \text{Al}_2\text{O}_3$  has a tendency to form the normal spinel configuration, where  $\text{Mg}^{2+}$  ions and  $\text{Al}^{3+}$  ions occupy mainly the tetrahedral and the octahedral sites, respectively. Electron irradiation induces simple cation disordering between the tetrahedral sites and the octahedral sites in  $\text{MgO} \cdot \text{Al}_2\text{O}_3$ . In addition to cation disordering, slight evacuation of cations from the tetrahedral sites to the octahedral sites occurs in a peak-damaged area in  $\text{MgO} \cdot \text{Al}_2\text{O}_3$  irradiated with  $\text{Ne}^+$  ions. In contrast, cation disordering is suppressed in  $\text{MgO} \cdot 2.4\text{Al}_2\text{O}_3$  irradiated with electrons. The structural vacancies, present in the non-stoichiometric compound, appear to be effective in promoting irradiation damage recovery through interstitial–vacancy recombination. © 2000 Elsevier Science B.V. All rights reserved.

## 1. Introduction

Magnesium aluminate spinel  $\text{MgO} \cdot n\text{Al}_2\text{O}_3$  exhibits strong resistance to formation of defect clusters under irradiation with high energy particles and it is expected to be an excellent candidate for insulators in the fusion reactors [1,2]. For example, no defect clusters have been observed under irradiation with 1 MeV electrons up to a few displacements per atom (dpa) in a wide temperature range [3–5]. The reliable stability in radiation fields is believed to come from a high rate of interstitial–vacancy recombination. It is partly because the spinel structure has a number of vacant sites. In the ideal ‘normal’ structure of stoichiometric case,  $\text{Mg}^{2+}$  and  $\text{Al}^{3+}$  ions occupy 1/8 of the tetrahedral sites and 1/2 of the octahedral ones, respectively, in the fcc lattice formed with  $\text{O}^{2-}$  ions. The rest positions remain as unoccupied sites in the lattice. In the non-stoichiometric cases with  $n > 1$ ,

a significant number of structural vacancies are introduced in the cation sites. Under irradiation conditions, it is expected that the recombination of  $\text{Mg}^{2+}$  and  $\text{Al}^{3+}$  ions with vacancies or the exchange of  $\text{Mg}^{2+}$  and  $\text{Al}^{3+}$  ions on their respective lattice sites will be readily accommodated. Cation disordering in  $\text{MgO} \cdot n\text{Al}_2\text{O}_3$  irradiated with neutrons has been quantitatively examined by means of neutron diffraction [6], and nuclear magnetic resonance [7]. These techniques, however, are thought to be unsuitable for the study of local microstructure in irradiated materials.

The purpose of the present study is to measure the site distribution of cations on the tetrahedral and the octahedral sites in  $\text{MgO} \cdot n\text{Al}_2\text{O}_3$  by electron channeling enhanced X-ray microanalysis. The technique takes advantage of the ALCHEMI (atom location by channeling enhanced microanalysis) technique [8]. The early formulation of ALCHEMI [9] leads to significant systematic errors in the site distributions of compounds consisting of light elements [10]. However, recent improvement with correction of the delocalization effect [11,12] has made ALCHEMI a reliable technique. In this study, we applied the technique to  $\text{MgO} \cdot n\text{Al}_2\text{O}_3$  before and irradiated with 900 keV electrons or 1 MeV  $\text{Ne}^+$  ions at 873 K.

\* Corresponding author. Tel.: +81-92 642 3771; fax: +81-92 642 3771.

E-mail address: soeda@regroup5.nucl.kyushu-u.ac.jp (T. Soeda).

2. Experimental procedure

For 900 keV electron irradiation, transmission electron microscope (TEM) specimens of  $MgO \cdot nAl_2O_3$  single crystals with  $n=1.0$  (Union Carbide) and 2.4 (Nakazumi Crystal) were dimpled to be 30  $\mu m$  thick and ion-milled with 5 keV  $Ar^+$  ions to electron transparency. They were annealed at 1470 K in a furnace for 48 h to remove lattice defects produced by ion milling, and then subsequently cooled. The specimens were irradiated at 870 K with 900 keV electrons to a dose of about 2 dpa ( $\phi_e t = 1.6 \times 10^{27} e/m^2$ ). For 1 MeV  $Ne^+$  ion irradiation, bulk  $MgO \cdot Al_2O_3$  was irradiated at 870 K to a dose of about 2 dpa ( $\phi_i t = 4.5 \times 10^{20} Ne/m^2$ ). The irradiated specimens were mechanically polished with a tripod polisher to a wedge shape. The specimens were examined with Philips EM420T (Argonne National Laboratory) operated at 120 kV and Philips CM200 (Oak Ridge National Laboratory) operated at 200 kV, equipped with an EDAX 9900 microanalyzer system. The influence of the electron irradiation on displacement damage during analysis can be ignored, since constituent atoms are hardly displaced out of their occupied sites below 250 kV. The angular resolution measurements of X-ray emission were carried out with incident beam rocking between  $-4g$  and  $+4g$  ( $g=400$ ) Bragg conditions.

3. Analytical procedure

We assume that  $O^{2-}$  ions form an ideal fcc sublattice in the spinel structure, and  $Mg^{2+}$  and  $Al^{3+}$  ions reside on part of the tetrahedral and octahedral sites. The occupation probabilities  $P_i$ s of  $Mg^{2+}$  and  $Al^{3+}$  on the tetrahedral sites are defined as parameters characterizing the structure. Table 1 gives relative numbers of these elements on the two cation sublattices in terms of  $P_i$ s.

Fig. 1(a) shows an example of electron channeling enhanced X-ray intensity variations as functions of incident beam tilting along the 400 direction. In the hor-

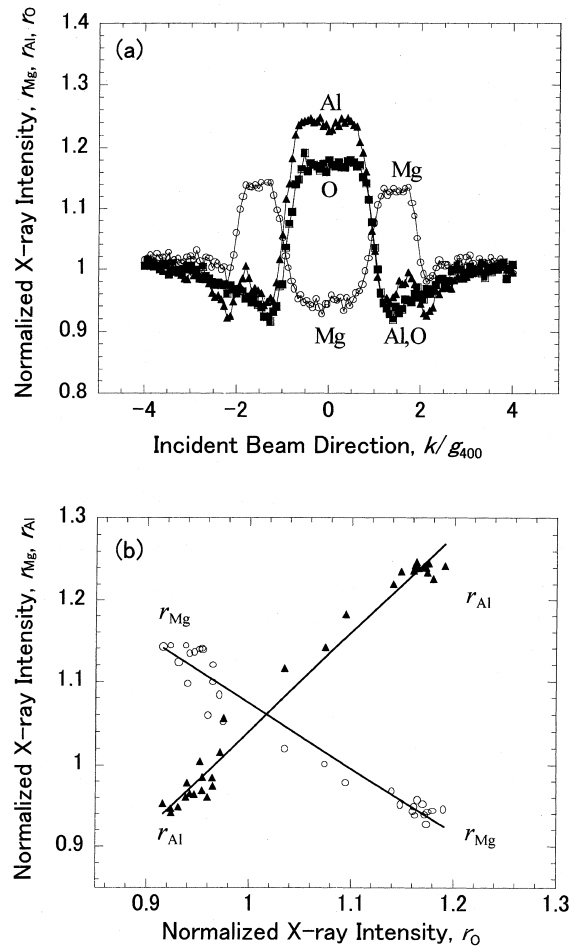


Fig. 1. An example of the characteristic X-ray intensity variations as a function of diffraction condition (a) and the response of the X-ray intensities of Mg K and Al K to O K; (b) in  $MgO \cdot Al_2O_3$ . Here  $k/g_{400}$  corresponds to the exact Bragg position for 400.

izontal axis,  $k/g_{400}=1$  corresponds to the exact Bragg condition for 400 reflection. Fig. 1(b) is obtained by re-plotting the X-ray intensities of Mg K and Al K as a

Table 1  
Numbers of ions and vacancies at the crystal sites per unit cell

	Tetrahedral site	Octahedral site	fcc Site	Total
$N_{Mg}$	$\frac{32}{3n+1} P_{Mg}$	$\frac{32}{3n+1} (1 - P_{Mg})$		$\frac{32}{3n+1}$
$N_{Al}$	$\frac{64n}{3n+1} P_{Al}$	$\frac{64n}{3n+1} (1 - P_{Al})$		$\frac{64n}{3n+1}$
$N_O$			32	32
$N_V$	$8 - (N_{Mg}^{IV} + N_{Al}^{IV})$	$16 - (N_{Mg}^{VIII} + N_{Al}^{VIII})$		
Total	8	16	32	

function of the intensity of O K. Here,  $r_i$  ( $i = \text{O, Mg or Al}$ ) is the ratio of the X-ray intensity under the dynamical condition to that under random condition in  $i$ -element. Indicated in Fig. 1(b) that a linear response of  $r_{\text{Mg}}$  and  $r_{\text{Al}}$  to  $r_{\text{O}}$  appears. Around the Bragg position of 400,  $r_{\text{O}}$  vary in terms of  $r_{\text{Mg}}$  and  $r_{\text{Al}}$ , according to

$$r_{\text{O}} = \frac{1}{1 - P_{\text{Al}}/P_{\text{Mg}}} \frac{1}{L_{\text{AlO}}} r_{\text{Al}} - \frac{P_{\text{Al}}/P_{\text{Mg}}}{1 - P_{\text{Al}}/P_{\text{Mg}}} \frac{1}{L_{\text{MgO}}} r_{\text{Mg}}, \quad (1)$$

where  $L_{\text{AlO}}$  and  $L_{\text{MgO}}$  are the coefficients for distribution of charge density in  $\text{Al}^{3+}$  ions or  $\text{Mg}^{2+}$  ions to  $\text{O}^{2-}$  ions, respectively, and can be measured experimentally as the ratio of  $r_{\text{Al}}$  and  $r_{\text{Mg}}$  to  $r_{\text{O}}$  at a 440 reflection. The values of  $P_{\text{Mg}}$  and  $P_{\text{Al}}$  were determined by comparing the angular dependent X-ray emission profiles with theoretical calculation based on the dynamical diffraction theory [13,14]. The numbers of  $\text{Mg}^{2+}$  ions and  $\text{Al}^{3+}$  ions per unit cell were evaluated from the occupation probabilities  $P_{\text{Mg}}$  and  $P_{\text{Al}}$ . The number of vacancies was then determined on the site conservation law for each site.

#### 4. Results and discussion

Table 2 lists the occupation probabilities of cations on the tetrahedral (T) and the octahedral (O) sites in

unirradiated  $\text{MgO} \cdot n\text{Al}_2\text{O}_3$ . In the case of  $\text{MgO} \cdot \text{Al}_2\text{O}_3$ , 90% of  $\text{Al}^{3+}$  ions are located on the O-sites, while 60% of  $\text{Mg}^{2+}$  ions are on the T-sites. This means that the compound has a tendency to form the normal spinel configuration. However, about 40% of  $\text{Mg}^{2+}$  ions and about 10% of  $\text{Al}^{3+}$  ions are located on the opposite sites. The partial disordering tendency of  $\text{Mg}^{2+}$  ions has been also revealed by neutron diffraction [6] as  $P_{\text{Mg}} = 0.763 \pm 0.02$  and  $P_{\text{Al}} = 0.118 \pm 0.01$ , and has been explained in terms of ionic size and induced lattice strain around the T-sites. Table 2 also shows the total number of ions in T-sites is less than 8 and that in O-sites is greater than 16 per unit cell. It suggests that some cations should occupy empty sites of octahedral positions in the spinel structure, resulting in the same amount of vacancies in the T-sites. In  $\text{MgO} \cdot 2.4\text{Al}_2\text{O}_3$ , in contrast, 27% of  $\text{Mg}^{2+}$  ions and 20% of  $\text{Al}^{3+}$  ions occupy the T-sites. It is indicated in Table 2 that the structural vacancies are predominantly located on the T-sites.

Table 3 shows the results of the occupation numbers of  $\text{Mg}^{2+}$  and  $\text{Al}^{3+}$  ions per unit cell on the T-sites and the O-sites in  $\text{MgO} \cdot n\text{Al}_2\text{O}_3$  after irradiation at 870 K with 900 keV electrons up to 2 dpa in a peak-damaged area. Here, the unirradiated area was about 1.2  $\mu\text{m}$  away from the periphery of the illuminated area. In  $\text{MgO} \cdot \text{Al}_2\text{O}_3$ , both  $\text{Mg}^{2+}$  and  $\text{Al}^{3+}$  ions have a tendency to replace their sites to the opposite sites, whereas the number of vacancies hardly changes by irradiation. This

Table 2

Occupation numbers of  $\text{Mg}^{2+}$ ,  $\text{Al}^{3+}$  and vacancies on the T-sites and the O-sites in a unit cell in  $\text{MgO} \cdot n\text{Al}_2\text{O}_3$  before irradiation<sup>a</sup>

		Number of ions		$P_i$
		T-sites (8)	O-sites (16)	
$n = 1.0$	$\text{Mg}^{2+}$	$4.9 \pm 0.1$	$3.1 \pm 0.1$	$0.61 \pm 0.01$
	$\text{Al}^{3+}$	$1.6 \pm 0.3$	$14.4 \pm 0.3$	$0.10 \pm 0.02$
	Vacancy	$1.5 \pm 0.3$	$\sim 0$	–
$n = 2.4$	$\text{Mg}^{2+}$	$1.1 \pm 0.1$	$2.8 \pm 0.1$	$0.27 \pm 0.01$
	$\text{Al}^{3+}$	$3.8 \pm 0.3$	$14.9 \pm 0.3$	$0.20 \pm 0.02$
	Vacancy	$3.2 \pm 0.4$	$\sim 0$	–

<sup>a</sup>The occupation probabilities on the T-sites ( $P_i$ ) are also tabulated.

Table 3

Occupation numbers of  $\text{Mg}^{2+}$ ,  $\text{Al}^{3+}$  and vacancies on the T-sites and the O-sites in the unirradiated area and the damaged area in  $\text{MgO} \cdot n\text{Al}_2\text{O}_3$  irradiation with 900 keV electrons to 2 dpa at 870 K<sup>a</sup>

		$N$	Unirradiated area		Damaged area	
			T-sites	O-sites	T-sites	O-sites
$n = 1.0$	$\text{Mg}^{2+}$	8.0	$3.9 \pm 0.1$	$4.1 \pm 0.1$	$2.2 \pm 0.1$	$5.8 \pm 0.1$
	$\text{Al}^{3+}$	16.0	$1.3 \pm 0.3$	$14.7 \pm 0.3$	$3.2 \pm 0.3$	$12.8 \pm 0.3$
	Vacancy	0.0	$2.9 \pm 0.3$	$\sim 0$	$2.6 \pm 0.3$	$\sim 0$
$n = 2.4$	$\text{Mg}^{2+}$	3.9	$1.1 \pm 0.1$	$2.8 \pm 0.1$	$1.1 \pm 0.1$	$2.8 \pm 0.1$
	$\text{Al}^{3+}$	18.7	$3.8 \pm 0.4$	$14.9 \pm 0.4$	$4.3 \pm 0.4$	$14.4 \pm 0.4$
	Vacancy	1.4	$3.2 \pm 0.3$	$\sim 0$	$2.6 \pm 0.3$	$\sim 0$

<sup>a</sup>The probabilities are given in terms of the number of ions per unit cell ( $N$ : total numbers of ions in a unit cell).

result indicates that simple cation disordering ensues in  $\text{MgO} \cdot \text{Al}_2\text{O}_3$ . In contrast,  $\text{Al}^{3+}$  ions increase and vacancies decrease in the T-sites in the damaged area in  $\text{MgO} \cdot 2.4\text{Al}_2\text{O}_3$ , while the number of  $\text{Mg}^{2+}$  ions on the T-sites hardly changes. It is suggested that displaced cations are mainly combined with structural vacancies on the T-sites. Namely,  $\text{Al}^{3+}$  ions directly combine with structural vacancies on the T-sites, or  $\text{Mg}^{2+}$  ions move to the O-sites by irradiation and then recombine with structural vacancies on the T-sites. The high concentration of structural vacancies would lead to the high rate of recombination, less disordered atomic arrangement and efficient suppression of the nucleation of interstitial loops [15].

Fig. 2 shows an example of the microstructure in  $\text{MgO} \cdot \text{Al}_2\text{O}_3$  irradiated with 1 MeV  $\text{Ne}^+$  ions at 870 K in the pre-peak damaged area (a), the peak damaged area (b) and the unirradiated area (c). The dose reaches about

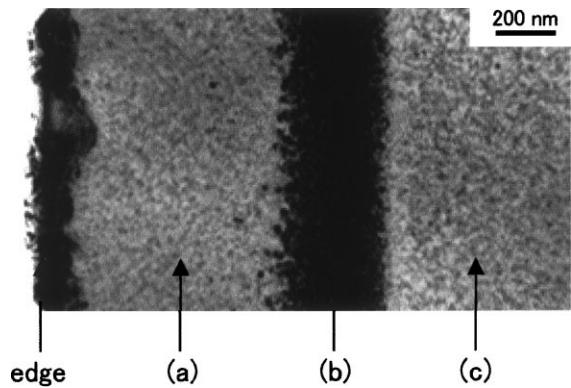


Fig. 2. Microstructure and diffraction patterns of  $\text{MgO} \cdot \text{Al}_2\text{O}_3$  irradiated at 870 K with 1 MeV  $\text{Ne}^+$  ions: (a) the pre-peak damaged area; (b) the peak damaged area and (c) the unirradiated area.

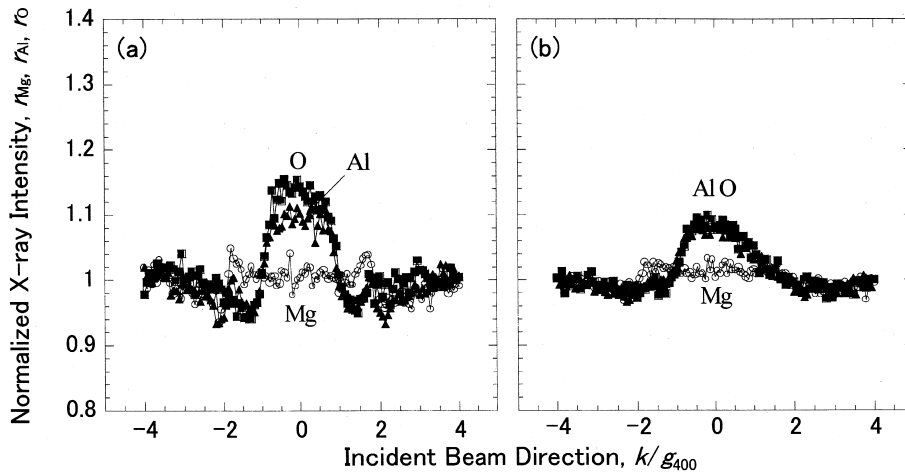


Fig. 3. X-ray intensity profiles of  $\text{MgO} \cdot \text{Al}_2\text{O}_3$  irradiated at 870 K with (a) 1 MeV  $\text{Ne}^+$  ions in the pre-peak damaged area and (b) the peak damaged area.

Table 4

Occupation numbers of  $\text{Mg}^{2+}$ ,  $\text{Al}^{3+}$  and vacancies on the T-sites and the O-sites after irradiation with 1 MeV  $\text{Ne}^+$  ions at 870 K in  $\text{MgO} \cdot \text{Al}_2\text{O}_3$  up to 2 dpa in the pre-peak damaged area<sup>a</sup>

$n = 1.0$		$N$	Occupation numbers	
			T-sites	O-sites
Unirradiated area	$\text{Mg}^{2+}$	8.0	$4.9 \pm 0.1$	$3.1 \pm 0.1$
	$\text{Al}^{3+}$	16.0	$1.6 \pm 0.3$	$14.4 \pm 0.3$
	Vacancy	0.0	$1.5 \pm 0.3$	$\sim 0$
Pre-peak damaged area	$\text{Mg}^{2+}$	8.0	$3.0 \pm 0.1$	$5.0 \pm 0.1$
	$\text{Al}^{3+}$	16.0	$3.5 \pm 0.3$	$12.5 \pm 0.3$
	Vacancy	0.0	$1.5 \pm 0.3$	$\sim 0$
Peak damaged area	$\text{Mg}^{2+}$	8.0	$3.0 \pm 0.1$	$5.0 \pm 0.1$
	$\text{Al}^{3+}$	16.0	$2.9 \pm 0.3$	$13.1 \pm 0.3$
	Vacancy	0.0	$2.2 \pm 0.3$	$\sim 0$

<sup>a</sup> The probabilities are given in terms of the number of ions per unit cell ( $N$ : total numbers of ions in an unit cell).

2 dpa in the pre-peak damaged area. Fig. 3 shows the electron channeling enhanced X-ray intensity profiles from the pre-peak damaged area (a) and the peak damaged area (b). The profiles change significantly compared with Fig. 1(a) for an unirradiated area, revealing that 1 MeV Ne<sup>+</sup> ion irradiation induces atomic re-arrangement.

Table 4 summarizes the occupation numbers of Mg<sup>2+</sup> ions and Al<sup>3+</sup> ions on the T-sites and the O-sites in MgO·Al<sub>2</sub>O<sub>3</sub> after irradiation at 870 K with 1 MeV Ne<sup>+</sup> ions. Indicated in Table 4 that the number of Mg<sup>2+</sup> ions decreases and that of Al<sup>3+</sup> ions increases on the T-sites in the pre-peak damaged area. Therefore, we conclude that simple cation disordering ensues in the pre-peak damaged area. This is thought to be reasonable because light ion irradiation significantly enhances point defect diffusion by large amount of ionization [16] in the pre-peak damaged area and promotes cation disordering during the irradiation. In the peak damaged area, in contrast, the total number of cations on the T-sites decreases and that of vacancies increases in comparison with the pre-peak damaged area. It results from that some of Al<sup>3+</sup> ions are displaced out of the T-sites to the O-sites. As a result, excess vacancies are produced on the T-sites in the peak damaged area. Neutron diffraction of MgO·Al<sub>2</sub>O<sub>3</sub> has suggested that a considerable amount of ions are located on the unoccupied sites of the octahedral positions after neutron irradiation up to 56 dpa at 678 K [6]. Heavy irradiation with 400 keV Xe<sup>2+</sup> or 1.5 MeV Kr<sup>+</sup> ions at cryogenic temperatures lower than 100 K [17–20] results in extinction of 220 reflections, which indicates evacuation of ions from the T-sites. These experimental results on heavily irradiation cases are qualitatively consistent with the present result in the peak damaged area. An extended study in MgO·nAl<sub>2</sub>O<sub>3</sub> irradiated with ions on other conditions is now being conducted.

## 5. Conclusion

Magnesium aluminate spinel MgO·nAl<sub>2</sub>O<sub>3</sub> ( $n = 1.0$  and 2.4) was examined by electron channeling enhanced X-ray microanalysis, in order to study a cation configuration before and after irradiation with 900 keV electrons or 1 MeV Ne<sup>+</sup> ions at 873 K. The non-stoichiometric compound showed more resistance to radiation damage than the stoichiometric one in terms of the stability of the cation configuration under irradiation. The present results imply that the high concentration of structural vacancies, present in non-stoichiometric compound, should be effective in

promoting irradiation damage recovery by interstitial–vacancy recombination.

## Acknowledgements

The authors should like to express their gratitude to Dr Lynn Rehn for arrangements for this collaborative work of the two groups at KU and ANL, and Dr Ian Anderson for help in the operation of CM-200 at ORNL. This research was partly sponsored by the US Department of Energy under contract BES-MS W-31-109-Eng-38 and by the Grant-in-Aid for scientific research from the Ministry of Education, Science, Culture and Sports, Japan and from the Japan Society of Promotion of Science.

## References

- [1] F.W. Clinard Jr., G.F. Hurley, R.A. Youngman, L.W. Hobbs, *J. Nucl. Mater.* 133–134 (1985) 701.
- [2] S. Zinkle, C. Kinoshita, *J. Nucl. Mater.* 251 (1997) 200.
- [3] S.N. Buckley, *J. Nucl. Mater.* 141–143 (1986) 387.
- [4] S.N. Buckley, S.J. Shaibani, *Philos. Mag. Lett.* 55 (1987) 15.
- [5] C. Kinoshita, K. Nakai, *Jpn. J. Appl. Phys. Series 2* (1989) 105.
- [6] K.E. Sickafus, A.C. Larson, N. Yu, M. Nastasi, G.W. Hollenberg, F.A. Garner, R.C. Bradt, *J. Nucl. Mater.* 219 (1995) 128.
- [7] E.A. Cooper, C.D. Hughes, W.L. Earl, K.E. Sickfufus, G.W. Hollenberg, F.A. Garner, R.C. Bradt, *Mater. Res. Soc. Symp. Proc.* 373 (1995) 413.
- [8] J.C.H. Spence, J. Taft, *J. Microsc.* 130 (1983) 147.
- [9] K.M. Krishnan, *Ultramicrosc.* 24 (1988) 125.
- [10] P.R. Munroe, I. Baker, *J. Mater. Res.* 7 (1992) 2119.
- [11] M.G. Walls, *Microsc. Microanal. Microstruct.* 3 (1992) 443.
- [12] I.M. Anderson, *Acta Mater.* 45 (1997) 3897.
- [13] C.J. Rossouw, C.T. Forwood, M.A. Gibson, P.R. Miller, *Micron* 28 (1997) 125.
- [14] L.J. Allen, T.W. Josefsson, C.J. Rossouw, *Ultramicrosc.* 55 (1994) 258.
- [15] K. Fukumoto, C. Kinoshita, S. Maeda, K. Nakai, *Nucl. Instrum. and Meth. B* 91 (1994) 252.
- [16] S.J. Zinkle, *Nucl. Instrum. and Meth. B* 91 (1994) 234.
- [17] K.E. Sickafus, N. Yu, R. Devanathan, M. Nastasi, *Nucl. Instrum. and Meth. B* 106 (1995) 573.
- [18] N. Bordes, K.E. Sickafus, E.A. Cooper, R.C. Ewing, *J. Nucl. Mater.* 225 (1995) 318.
- [19] R. Devanathan, K.E. Sickafus, N. Yu, M. Nastasi, *Philos. Mag. Lett.* 72 (1995) 155.
- [20] N. Yu, R. Devanathan, K.E. Sickafus, M. Nastasi, *J. Mater. Res.* 12 (1997) 1766.